Citation: BoneKEy Reports **4**, Article number: 662 (2015) | doi:10.1038/bonekey.2015.29

www.nature.com/bonekey

REVIEW

Assessment of bone vascularization and its role in bone remodeling

Marie-Hélène Lafage-Proust[1,2], Bernard Roche[1,2], Max Langer[2,3], Damien Cleret[1,2], Arnaud Vanden Bossche[1,2], Thomas Olivier[2,4] and Laurence Vico[1,2]

[1]Laboratoire de Biologie Intégrée du Tissu Osseux, INSERM U 1059, Saint-Etienne, France. [2]Université de Lyon, Lyon, France. [3]CREATIS, CNRS UMR 5220-INSERM U1044, Lyon, France. [4]Laboratoire Hubert Curien, Saint-Etienne, France.

Bone is a composite organ that fulfils several interconnected functions, which may conflict with each other in pathological conditions. Bone vascularization is at the interface between these functions. The roles of bone vascularization are better documented in bone development, growth and modeling than in bone remodeling. However, every bone remodeling unit is associated with a capillary in both cortical and trabecular envelopes. Here we summarize the most recent data on vessel involvement in bone remodeling, and we present the characteristics of bone vascularization. Finally, we describe the various techniques used for bone vessel imaging and quantitative assessment, including histology, immunohistochemistry, microtomography and intravital microscopy. Studying the role of vascularization in adult bone should provide benefits for the understanding and treatment of metabolic bone diseases.

BoneKEy Reports **4**, Article number: 662 (2015) | doi:10.1038/bonekey.2015.29

Introduction

The skeleton is an adaptable system that integrates a number of mechanical, biochemical and nervous signals. Moreover, bone is a feedback controlled composite organ that fulfils several interconnected functions including locomotion, involvement in phosphate and calcium metabolism, synthesis of endocrine molecules and hematopoiesis, which may conflict with each other in pathological conditions. Bone vascularization is at the interface between these functions. As for other organs, blood flow within a bone is tightly correlated with its metabolic activity: by controlling oxygen and nutrient delivery, bone vessels become a limiting factor, which may alter the various physiological functions of bone and could potentially modulate treatment efficacy in metabolic bone diseases. Hemodynamics, oxygen consumption and energetic metabolism are intimately coupled with the activities of bone formation and resorption during bone modeling and remodeling. The roles of vessels have been well documented in various bone modeling situations. Blood vascular penetration into the avascular cartilage template is a landmark of the early steps of endochondral ossification, and the invasion by blood vessels of the growth plate hypertrophic zone is an essential event for bone elongation.[1] The development of a new vascular network is a critical step in wound healing and represents a primary limiting factor in functional tissue regeneration.[2] Overall, bone modeling is characterized by a tightly regulated positive coupling between osteogenesis and angiogenesis. Therefore, bone vascularization has become a relevant therapeutic target in both fields of fracture repair[3] and bone tissue engineering.[4] In contrast, the relationships between vessels and bone remodeling remain poorly understood. In this review, we summarize the current knowledge on the role of vessels in bone remodeling and briefly describe the various techniques available for bone vessel identification and quantification. The methods for assessment of bone blood perfusion are beyond the scope of this review.

The Role of Vessels in Bone Remodeling

Within cortices, the remodeling cutting and closing cones, which build secondary osteons, are centered by a vessel (**Figure 1**; bottom). It is necessary to stress that mice and rats lack a well-developed Haversian remodeling system and mostly lose cortical bone at the endosteum, in contrast to larger mammals whose increased Haversian remodeling is a major cause of cortical porosity and age-related bone loss. In humans, Haversian vascular canals are roughly parallel to the diaphysis axis and highly connected at right angle to 'Volkman' canals. In the mouse, canals exhibit a radial pattern and are poorly branched (as shown by Schneider *et al.*[5]), whereas in the rat, they are more interconnected and oriented like in humans (**Figure 2**)[6]. Thus, the organization of cortical vascularization in long bones strongly differs among species. As a result, the role

Correspondence: Professor M-H Lafage-Proust, Laboratoire de Biologie Intégrée du Tissu Osseux, INSERM U 1059, Saint-Etienne 42023, France.
E-mail: lafagemh@univ-st-etienne.fr

Received 9 May 2014; accepted 4 February 2015; published online 8 April 2015

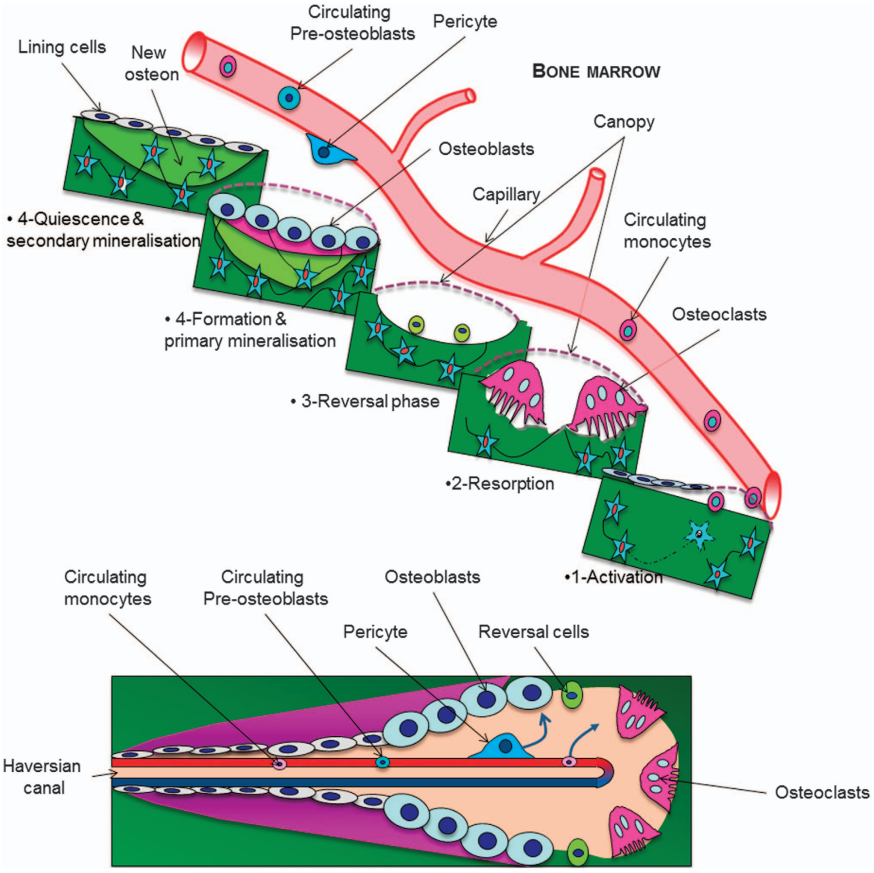

Figure 1 Illustration of spatial and functional relationships between blood capillary and the bone remodeling compartment in trabecular (top) and cortical envelopes (bottom). Circulating osteoclast precursors home to the bone surface through the vessel wall and the canopy where the bone remodeling unit is about to take place. The vessel also feeds the bone remodeling compartment with osteoblast progenitors via pericytes borne by the vascular wall or via circulating cells.

of vessels in physiological cortical bone remodeling and in pathological conditions may not be strictly comparable between models.

In contrast to cortical bone, diagrams illustrating trabecular bone remodeling drawn 20 years ago constantly lacked the bone vessel. However, those designed more recently repeatedly show a capillary close to the remodeling unit (http://stemcells.nih.gov/info/2006report/chapter11.htm). Indeed, there is accumulating evidence that the bone vasculature is a crucial partner in the bone remodeling process and has a role in the resorption/formation coupling. Bone vessels bring osteoclast precursors at the bone surface where remodeling is about to take place and 'feed' the remodeling unit with new cells as long as necessary (**Figure 1**). As for the osteoblastic lineage, studies suggest that osteoprogenitors could be recruited from circulating cells,[7] differentiated from pericytes,[8,9] or from cells located in the canopy[10] that isolate the bone remodeling compartment from the bone marrow[11,12] (**Figure 1**; top). Interestingly, canopy cells are in close contact with capillaries and Delaissé's team recently demonstrated that vessel positioning relative to the bone surface was highly dependent on the remodeling status of the bone remodeling compartment,[13] suggesting substantial vessel plasticity. The complex molecular crosstalk between bone and vascular cells (reviewed in reference 14) is progressively unraveled and includes the cues involved in angiogenesis, such as vascular endothelial growth factor receptor[15] or preosteoclasts/preosteoblasts homing, such as Sphingosine-phosphate 1 concentrations[16] or CXCR4/CXCL12 signaling,[17,18] which control cell trafficking through the vascular wall.

Recently, Kusumbe *et al.*[19] described two subtypes of bone vessels according to their high (H) or low (L) level of CD31 and endomucin expression. In young animals, H vessels contain more proliferating endothelial cells. They are abundant in the primary spongiosa and run along the cortical endosteum. H vessels are more surrounded with osteoprogenitors, express higher levels of HIF-1α but are less numerous than L-type vessels. Most interestingly, inhibition or activation of the HIF-1α signaling pathway in endothelial cells only modulates bone mass and perivascular osteoprogenitor number. Genetic lineage tracing showed that H endothelial cells mediate neoangiogenesis in bone. The amount of H endothelial cells declines with age in the bone marrow, whereas that of total endothelial cells does not. Deferoxamin treatment, which stabilizes HIF-1α, was osteogenic and led to substantial expansion of type H endothelium and emergence of vessel-associated osteoprogenitors in aged animals. Xie *et al.*[20] further showed that platelet-derived growth factor-BB, exogenous or released by preosteoclasts, induces type H vessel and stimulates bone formation in OVX mice. Altogether, these exciting data emphasize the high heterogeneity of bone vasculature and clearly identify the bone vessel as a therapeutic target in metabolic bone diseases. However, the kinetics of vessel behavior during the whole remodeling process (activation,

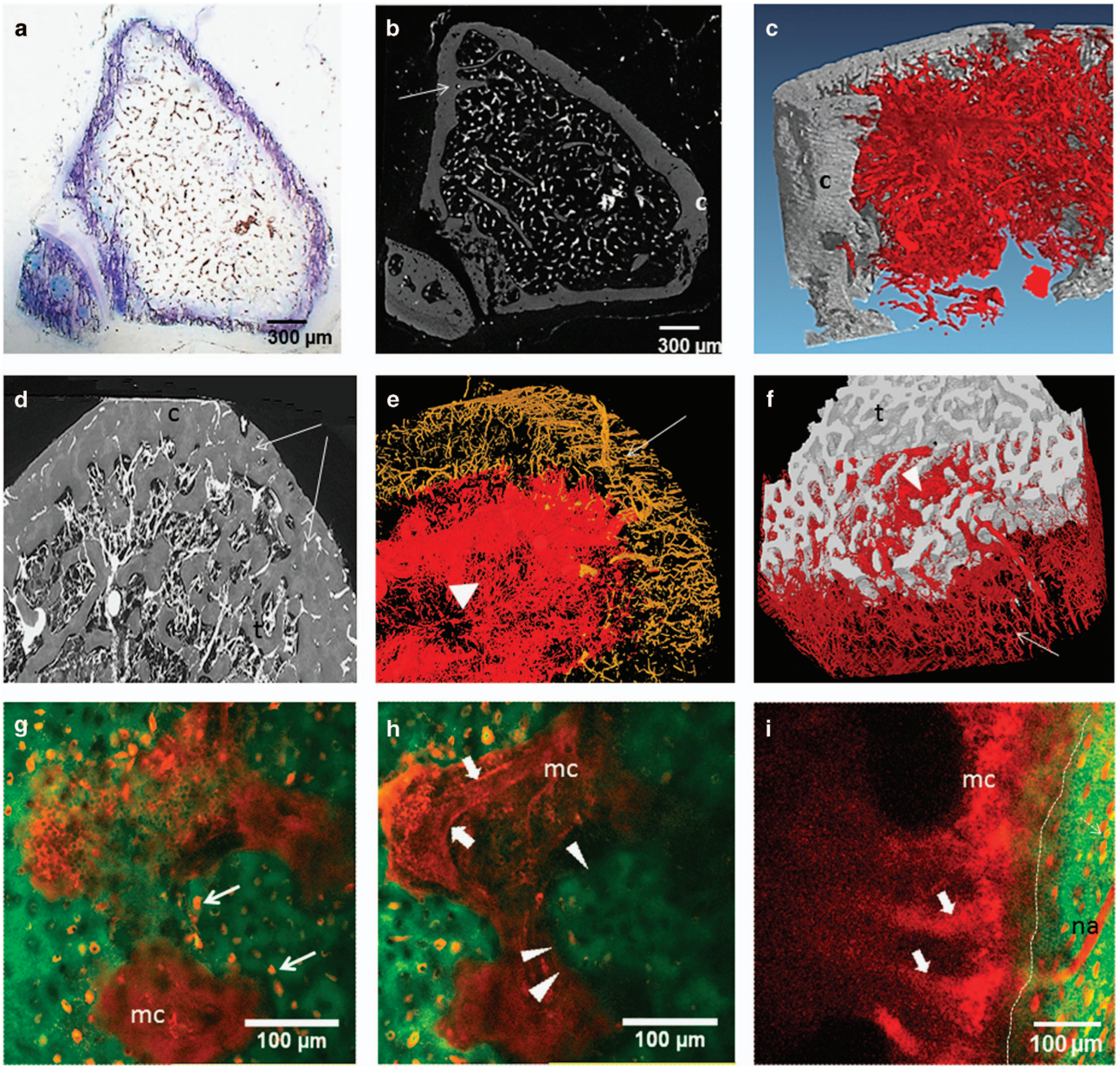

Figure 2 (**a**–**f**) Imaging of barium-infused vessels in tibia of mice (**a**–**c**) and rats (**d**–**f**). Arrows: cortical vessels, arrow head: trabecular vascular network. t, trabecular bone; c, cortical bone. (**a**) Horizontal toluidine blue-stained 5-µm-thick section of barium-infused mouse tibia upper metaphysis. (**b**) Micro-CT image (3-µm resolution, Nanotom, GE Inspection Technology, Boston, MA, USA) of the same tibia section illustrated in **a**. (**c**) 3D rendering of synchrotron radiation microtomography (SR-CT) of the vascular network in mouse tibia upper metaphysis (1.5-µm resolution). (**d**) Seventy-µm-thick stack of SR-CT images of rat upper tibia metaphysis. (**e**) 3D rendering of SR-CT imaging of cortical (yellow) and trabecular vascular network (red) in tibia diaphysis after segmentation and removal of the bone component. (**f**) 3D rendering of SR-CT imaging of cortical and trabecular vascular network (red) after segmentation and removal of the cortical bone component. (**g**–**i**) Intravital microscopy of Rhodamine B dextran-infused vessels in mouse calvaria (**g**, **h**) and tibia metaphysis (**i**). Performed on anesthetized mouse after incision of the skin and slight grinding of the cortical bone (tibia), 10 min after IV injection in the tail vein of Rhodamine B dextran with the Two-photon confocal microscope TCS-SP2, Leica Microsystems. (**d**, **e**) Two z-images of the same field separated by 50 µm, **d** being more superficial than **e**. Green: second-harmonic generation signals derived from bone collagen. Thin arrows: Rhodamine-filled osteocyte lacunae, thick arrows: Rhodamine–dextran-filled capillary (note the red blood cells inside the vessel), arrow heads and dotted line: endocortical surface. mc, marrow cavity; na, nutrient artery in tibia; 3D, three-dimensional; IV, intravenous.

resorption, formation and quiescence, cf **Figure 1**) and the precise molecular mechanisms that control it remain unknown.

Involvement of Bone Vasculature in Metabolic Bone Diseases: Clinical Perspectives

Certainly, the abundant literature showing strong associations between osteoporosis and atherosclerosis or vascular calcifications led to the concept of the 'bone–vascular axis' suggesting common pathophysiological links between skeletal and vessel diseases,[21] especially in the ageing context. However, a limited number of studies specifically analyzed the connections between bone vascularization or perfusion and metabolic bone diseases in humans. Burkhardt *et al.*[22] found on histological sections that bone marrow vessels became increasingly scarce with age. In line with these morphological

findings, Wang and colleagues, using magnetic resonance imaging, reported a reduction in bone perfusion in post-menopausal osteoporotic women, as compared with age-matched healthy controls,[23] whereas a decrease in bone vascular density was observed in ovariectomized rodents.[24,25] Jumping to simplistic conclusions, one could think that 'the more vessels/perfusion, the better for bone'. However, although overexpression of vascular endothelial growth factor receptor in the chondro-osteoblast lineage in adult mice is angiogenic and increases trabecular bone mass, it also induces fibrotic marrow and cortical porosity, reminiscent of what is observed in secondary hyperparathyroidism.[1] Some non-malignant bone diseases are associated with complex vascular anomalies. Paget's disease and reflex sympathetic dystrophy at its early stage[26] both feature a significant increase in bone blood flow and accelerated resorption; however, the former leads to bigger bones, whereas the latter is associated with bone loss. These caricatural examples somehow emphasize the fact that the functional relationships between bone remodeling and vessels may not be as straightforward as previously thought.

Morphological and Functional Heterogeneity of Bone Vessels

Bone is highly vascularized. Sub-periosteal and bone marrow vessels are connected via the cortical vascular network. Bone marrow vessels are heterogeneous and include small « classic » capillaries ($<$10–15 μm) and a majority of sinusoid capillaries (20–30 μm), which belong to the venous capillary system. It is noteworthy that there is no lymphatic vessel in the normal bone marrow, whereas sub-periosteal lymphatic vessels run along the outer surface of the cortical bone.[27] Both classic capillary and sinusoid networks are linked by transitional vessels, which share some features of the vessels they connect to.[28] The basal membrane of sinusoids is absent or discontinuous. Their wall is perforated by inter- and intra-endothelial pores through which mature hematopoietic cells traffic towards the blood circulation, whereas intravascular soluble and relatively large molecules can be rapidly extravasated.[29]

Endothelial cells share basal membrane with pericytes, which are borne by the vessel wall. The pericyte vessel wall coverage is variable according to the type of vascular bed. Sixty-five percent and 71% of the adventitial sinusoid surface are covered by pericytes in the bone marrow of the rat[30] and the mouse,[31] respectively, this percentage being potentially reduced when egress of hematopoietic cells increases. In healthy humans older than 50 years, an average of 51% (±20%) of the bone marrow microvessels were reported to be covered by pericytes.[29]

Sinusoids and classic capillaries networks differ in terms of spatial organization. The sinusoid network is denser, isotropic and organized in a mesh-like structure, whereas the capillary bed has a tree-like shape. Finally, direct measurements at the endosteum of the rabbit fibula have shown that sinusoidal blood flow is only one-tenth of that in capillaries.[32] Expectedly, numerous sinusoids irrigate the 'red' hematopoietic marrow, whereas scarce classic capillaries are observed in the 'yellow' fatty marrow.[33–35] Using standard histological staining procedures of iliac crest biopsies from normal human subjects, Burkhardt *et al.* reported that the age-associated reduction in the capillary and sinusoid beds correlated with the overall increase in bone marrow fat volume.[20] In contrast, in the lower third of the diaphysis of rodents, a region filled with marrow adipocytes, we counted $>$100 vessels per mm^2, whereas there were 60–65 vessels per mm^2 in the metaphysis where the marrow is essentially hematopoietic.[36] These discrepancies underline that the relationships between bone adipocytes and vessels are complex, which may be related to the various subtypes of fat cells found in the marrow.[37]

We do not know whether there are variations in the vascular network structure or morphology throughout the skeleton in humans. In 4-month-old mice, we counted similar number of barium-infused microvessels in tibia and femur,[38] and, in younger mice, Lassailly *et al.*[39] did not find any difference in bone vessel densities between calvaria and long bones. Furthermore, these authors studied perfusion efficiency assessed after Ho 33342 dye perfusion followed by analysis of the bone marrow cell dye uptake. There was no difference in overall perfusion efficiency between long bone diaphyses, epiphyses and calvaria. However, truly hypoxic cells (as measured by pimonidazole staining that identifies cells exposed to oxygen partial pressure (PO_2) $<$10 mm Hg) were less frequent within calvaria as compared with long bones. Thus, although the bone marrow is highly vascularized, its perfusion is heterogeneous, some regions being poorly perfused and hypoxic, regardless of the type of bone. Recently, Spencer *et al.* were able to perform *in vivo* measurements of PO_2 using two-photon phosphorescence lifetime microscopy in mice. They found a PO_2 decreasing gradient from the periosteum (50 mm Hg) to the extravascular bone marrow compartment, with PO_2 as low as 9.9 mm Hg in this latter area. However, the peri-endosteal region (zone located at 0–20 μm from the bone surface) in which the smallest vessels were observed exhibited intermediate values (21.9 mm Hg in the vessels and 13.5 mm Hg outside the vessels).[40] A growing number of reports suggested a critical role of local hypoxia in the hematopoietic niche related to the stemness maintenance of the hematopoietic stem cells. These data emphasize the fact that vessel count cannot be a surrogate marker of blood supply or perfusion in bone and that the combination of morphological and functional analyses are necessary to better understand the bone/vessel relationship.

Methods for Assessment of Bone Vascularization

Assessment of bone vascularization requires visualization and identification of the vascular structures before their quantification. It consists in either labeling the vessel wall or filling the vascular network with a contrast product.

Vessel Wall Labeling

Vessel wall labeling can be performed via the use of reporter genes driven by endothelial-specific promoter, immunohistochemistry or intravenous injection of molecules captured by endothelial cells. Tie2[26] or VE Cadherin (also called Cadherin 5)[41] promoters may be employed in the mouse, considering that the Tie2 promoter is activated in classic capillaries and not in sinusoids.[26] Immunohistochemistry targets either endothelial cells (summarized in **Table 1**) or smooth muscle cells (anti-smooth muscle alpha-actin antibodies). In addition, functional properties of endothelial cells may be exploited for capillary detection such as endocytosis of

Table 1 Main endothelial markers used for identification of microvessels in the bone marrow of mice, rabbit and humans.

	Mice		*Humans*		
	Marrow sinusoids	*Marrow arteriolae/arterial capillaries*	*Marrow sinusoids*	*Marrow arteriolae/arterial capillaries*	*References*
Von Willebrand factor	−				Li *et al.*[28]
			+	+	Pusztaszeri *et al.*[76]
	+	+			Soki *et al.*[77]
CD31	−				Li *et al.*[28]
			+	+	Pusztaszeri *et al.*[76]
	+	+			Coenegrachts *et al.*[78]
	+	+			Van Valckenborgh *et al.*[71]
MECA32	+	+			Li *et al.*[28]
Laminin	+				Li *et al.*[28]
Tie2	−	+			Anghelina *et al.*[79]
Endomucin	+	−			Wang *et al.*[41]
Lectin	+	+			Li *et al.*[28]
Ac LDL	+	−			Li *et al.*[28]
CD34	±	+			Kristensen *et al.*[11]
			+	+	Pusztaszeri *et al.*[76]
VEGFR3	+	+			Singbrant *et al.*[74]

Abbreviation: VEGFR3, vascular endothelial growth factor receptor 3. Gray cells represent the antibodies able to differentiate sinusoids from capillaries.

fluorescent acetylated low-density lipoprotein (Dil-Ac-LDL)[26] or isolectin binding.[26] Li *et al.* combined the analysis of green fluorescent protein-Tie2 expressing capillaries and Dil-Ac-LDL endocytosis (sinusoids) to characterize the bone marrow vascular bed. They described 'transitional' microvessels interfacing and connected to the sinusoid and capillary networks whose specific function remains unknown. Wang *et al.* demonstrated that endomucin antibody specifically stains sinusoids as compared with the non-specific expression of VE Cadherin.[39] The pericytes can be identified with anti-platelet-derived growth factor receptor β, desmin or neuro-glial antigen 2 antibodies.[42] In addition, a growing body of studies reports expression of a various number of proteins (such as nestin,[43] leptin receptor[44] in mice or CD146[19] in humans) by subpopulations of pericytes, which are involved in the hematopoietic niche.

Most of the studies use 5-μm-thick cryosections and immunofluorescence, although some authors utilize decalcified paraffin-embedded samples with terrific results.[11,13] Recently, Adams' team published outstanding low magnification images of immunofluorescence-labeled vessels on 300-μm-thick frozen decalcified mouse whole tibia sections.[45] Finally, it is also possible to perform *in vivo* vessel labeling by intravascular injection of antibodies[46] or isolectin,[37] followed by *in vivo* or *ex vivo* confocal/multiphoton microscopy. After immunological staining, vessel quantification may be automated, sometimes preceded by manual tracking, provided that labeling is clean enough.[47]

Filling the Vascular Network with Contrast Product

Injection of fluorescent molecules and intravital microscopy. Branemark was the first to perform intravital microscopy of bone vascularization by observing under a microscope a trans-illuminated rabbit fibula.[48] The use of fluorescent probe intravenous injection combined with intravital microscopy of mouse calvaria was introduced by Von Andrian's team.[49] Two-photon fluorescence can be collected through the bone cortex via a confocal microscope as long as that the cortex is flat and thin enough, which makes mouse calvaria the best candidate for this imaging technique. After mouse anesthesia, fluorescent tracers (Rhodamine/fluorescein isothiocyanate-labeled dextran or smaller particles such as quantum dots) are injected into the blood circulation followed by observation under the confocal microscope. Under two-photon excitation, type 1 collagen is easily identified via second harmonics generation (**Figure 2g–i**). Using this technique, Lo Celso *et al.*[50] quantified the spatial relationships between bone marrow vessels, hematopoietic stem cells and green fluorescent protein (GFP)-runx$_2$-positive osteoblastic cells. Some authors insert a glass window in rodent femur after perforating the cortex, which allows longitudinal survey of bone vessels with time-lapsed imaging. Using this technique, trafficking of GFP-labeled preosteoclasts through the capillary walls could be markedly observed.[16] Grinding tibia cortex down to a 100 μm thickness permits to image the tibia marrow cavity[51] (**Figure 2g–i**).

Radio-opaque contrast product, histology and microtomography imaging

Choice of the contrast product. Pioneer anatomists and surgeons[52–54] used infusion of gelatin-india ink as a contrast product, followed by visualization of bone vessels on whole mounts or histological sections. This technique is still used for the analysis of cortical vessels in animal models.[55]

Later on, vascular corrosion casts were obtained after infusion and polymerization of methylmethacrylate resin followed by bone matrix digestion and scanning electron microscopy imaging. Beside resin, rubber such as latex can be infused; however, its molecular size and viscosity limit its penetration into the fine branches of the vascular network and only the primary arteries and a few of the larger secondary arterioles may be injected,[56] restricting its use to anatomy studies. This infusion technique can be used in human cadavers, rodents[57] or bigger animal models. Radio-opaque compounds such as barium sulfate or, more recently, lead chromate-loaded silicon (Microfil, Flow Tech, Inc., Carver, MA, USA) were used. They allow both histology and X-ray-based imaging including microtomography

(μCT). Microfil is suitable to image vessels outside the bone,[58] within muscles, as well as in soft organs. In contrast, we demonstrated that a barium sulfate solution (with barium particle size of 1–2 μm, Micropaque, Guerbet, Roissy, France) is a better tool for bone vessel visualization within trabecular bone in rodents, because it fully penetrates the marrow vessels including the smallest ones and it does not shrink after resin embedding[34] (**Figure 2**) as Microfil does. Indeed, most of the publications using Microfil opacification of bone marrow vessels show few ball-shaped vessels and discontinuous vascular networks.[59,60] In cortical bone, the vessels were reproducibly filled with barium in rats[61] (**Figure 2d–f**) but not in mice[34] (**Figure 2b**), probably because of inadequate rheology/output of the barium solution for infusion of mouse cortical vessels. In line with our results, Schneider *et al.*[62] quantified the cortical canal network before and after barium infusion and found that the volume of the vascular network was much smaller than that of the cortical porosity.

Microtomography imaging. Duvall *et al.*[63] thoroughly described the algorithms for μCT imaging of the vascular network in the rat hindlimb ischemic model and illustrated the influence of threshold levels on results. Using a similar approach with Scanco μCT devices (VivaCT and μCT40 Scanco Medical AG, Basserdorf, Switzerland), we analyzed the influence of both spatial resolution and threshold on trabecular bone vascularization in barium sulfate-infused rat tibiae after decalcification and found significant positive correlations between histology and μCT results.[64] Synchrotron radiation μCT imaging provided better spatial resolution compared with conventional μCT and did not require sample decalcification, thus allowing to visualize vessels in three-dimensions and analyze their location in relation to the bone surfaces.[61] Using an IMAGEJ-based software, we completed our analysis on histological sections by measuring the mean distance between vessels and the bone-forming surfaces (identified by the presence of osteoid) according to the vessel size. With these specific tools, we showed that intermittent PTH 1-84 was osteogenic but not angiogenic and relocated the smallest vessels closer to the bone-forming sites, in rats.[65] In mice, conventional μCT with 10-μm^3 voxel size is not suitable for bone vascular imaging even after sample decalcification.[34] As expected, 1.5-μm-thick slices obtained with synchrotron radiation μCT provided excellent contrast between vessels and trabeculae as did conventional μCT (Scanco μCT50 and GE nanoCT) with a 3-μm resolution (**Figure 2**). As said above, we were not able to fully infuse the cortical vascular network with barium sulfate solution in mice (as seen in **Figure 2**). Yet, it is possible, using μCT, to image the cortical porosity to assess the vascular cortical network, provided that the resolution is high enough.[66]

Bone Vascular Quantitative Assessment

Bone vessel quantification has been performed on three-dimensional μCT data sets from barium or Microfil-infused bones. Most of the teams use the software developed for measurements of trabecular bone, which generates parameters such as vascular volume per tissue volume (%), mean vessel thickness (μm) or separation and vessel number (/mm). Expectedly, numerical results depend on the quality of the image, which itself is contingent upon infusion conditions, leading to high variability of mouse bone marrow vessel densities among the studies. Vessel quantification can also be performed on histology or μCT images of immunohistochemistry stained or barium-filled vessels, respectively, by means of manual count (grid)[34] or semi-automatic[60] image analysis. Vascular volume per tissue volume (VV/TV, %) or per marrow volume (VV/Mar V,%) and mean vessel number per mm^2 of bone marrow area (V Nb/Mar Ar) are measured, and the mean vessel area (μm^2) is calculated by dividing the total vessel area (in μm^2) by vessel number.[34,67] Unfortunately, in contrast to the field of malignant diseases associated with bone marrow angiogenesis,[68] there is no methodological consensus on the parameter nomenclature and regions of interest for the quantification of bone marrow vessels. This leads to a pronounced heterogeneity of the results among the various publications. As an example, the vascular density in C57BL/6 mouse tibia or femur varies from 40[69] to 280[70] vessels per mm^2 of bone marrow with CD31 antibodies, from 20[71] to 150[72] per mm^2 with vascular endothelial growth factor receptor 3 antibodies, and was found as low as 10 per mm^2 with anti-CD34 antibodies in 6-month-old mice.[73] Furthermore, we were able to show that, beside differences in vessel count due to methodology, mouse genetic background, age and sex modulate the bone marrow vessel density.[34] These discrepancies may not influence the interpretation of the results within one study but make comparisons between studies difficult.

On the basis of synchrotron radiation μCT images of cortical bone, Schneider *et al.*[74] reported mouse strain and sex-related differences in vascular channel structure and density. In human bone, Cooper *et al.*[75], using skeletonization techniques were able to image and quantify the density and connectivity of the cortical 'vascular' porosity. Their work suggests that three-dimensional morphologic analysis of the canal network may provide novel insights into bone physiology that are not possible with two-dimensional approaches. Thus, intra-cortical porosity could serve as a surrogate parameter for assessing vascular density in this envelope. In contrast, measurement of vascular volume with this technique might be less accurate, the pore size being highly dependent on the resorption and formation periods.

Conclusion

Blood vessels exhibit tight structural and functional relationships with bone cells, which are not fully understood. A better understanding of vessel function improved the management of various diseases, which affect the kidney, heart or brain. Thus, studying the roles of vascularization in bone by the means of adequate tools and reproducible techniques should provide similar benefits for the comprehension and treatment of metabolic bone diseases.[76–78]

Conflict of Interest

The authors declare no conflict of interest.

References

1. Maes C. Role and regulation of vascularization processes in endochondral bones. *Calcif Tissue Int* 2013; **92**: 307–323.
2. Boerckel JD, Uhrig BA, Willett NJ, Huebsch N, Guldberg RE. Mechanical regulation of vascular growth and tissue regeneration in vivo. *Proc Natl Acad Sci USA* 2011; **108**: 674–680.
3. Street J, Bao M, de Guzman L, Bunting S, Peale Jr FV , Ferrara N *et al.* Vascular endothelial growth factor stimulates bone repair by promoting angiogenesis and bone turnover. *Proc Natl Acad Sci USA* 2002; **23**: 9656–9661.

4. Harris GM, Rutledge K, Cheng Q, Blanchette J, Jabbarzadeh E. Strategies to direct angiogenesis within scaffolds for bone tissue engineering. *Curr Pharm Des* 2013; **19**: 3456–3465.
5. Schneider P, Voide R, Stampanoni M, Donahue LR, Müller R. The importance of the intracortical canal network for murine bone mechanics. *Bone* 2013; **53**: 120–128.
6. Palacio-Mancheno PE, Larriera AI, Doty SB, Cardoso L, Fritton SP. 3D assessment of cortical bone porosity and tissue mineral density using high-resolution μCT: effects of resolution and threshold method. *J Bone Miner Res* 2014; **29**: 142–150.
7. Eghbali-Fatourechi GZ, Lamsam J, Fraser D, Nagel D, Riggs BL, Khosla S. Circulating osteoblast-lineage cells in humans. *N Engl J Med* 2005; **352**: 1959–1966.
8. Doherty MJ, Ashton BA, Walsh S, Beresford JN, Grant ME, Canfield AE. Vascular pericytes express osteogenic potential in vitro and in vivo. *J Bone Miner Res* 1998; **13**: 828–838.
9. Bianco P, Sacchetti B, Riminucci M. Osteoprogenitors and the hematopoietic microenvironment. *Best Pract Res Clin Haematol* 2011; **24**: 37–47.
10. Kristensen HB, Andersen TL, Marcussen N, Rolighed L, Delaisse JM. Osteoblast recruitment routes in human cancellous bone remodeling. *Am J Pathol* 2014r; **184**: 778–789.
11. Kristensen HB, Andersensen TL, Delaissé JM. Recruitment of osteoblasts in human cancellous bone remodeling. *Bone* 2012; **50**: S1–S65.
12. Parfitt AM. The mechanism of coupling: a role for the vasculature. *Bone* 2000; **26**: 319–323.
13. Kristensen HB, Andersen TL, Marcussen N, Rolighed L, Delaisse JM. Increased presence of capillaries next to remodeling sites in adult human cancellous bone. *J Bone Miner Res* 2013; **28**: 574–585.
14. Chim SM, Tickner J, Chow ST, Kuek V, Guo B, Zhang G *et al.* Angiogenic factors in bone local environment. *Cytokine Growth Factor Rev* 2013; **24**: 297–310.
15. Maes C, Goossens S, Bartunkova S, Drogat B, Coenegrachts L, Stockmans I *et al.* Increased skeletal VEGF enhances beta-catenin activity and results in excessively ossified bones. *EMBO J* 2010; **29**: 424–441.
16. Ishii M, Egen JG, Klauschen F, Meier-Schellersheim M, Saeki Y, Vacher J *et al.* Sphingosine-1-phosphate mobilizes osteoclast precursors and regulates bone homeostasis. *Nature* 2009; **458**: 524–528.
17. Zhang Q, Guo R, Schwarz EM, Boyce BF, Xing L. TNF inhibits production of stromal cell-derived factor 1 by bone stromal cells and increases osteoclast precursor mobilization from bone marrow to peripheral blood. *Arthritis Res Ther* 2008; **10**: R37.
18. Otsuru S, Tamai K, Yamazaki T, Yoshikawa H, Kaneda Y. Circulating bone marrow-derived osteoblast progenitor cells are recruited to the bone-forming site by the CXCR4/stromal cell-derived factor-1 pathway. *Stem Cells* 2008; **26**: 223–234.
19. Sacchetti B, Funari A, Michienzi S, Di Cesare S, Piersanti S, Saggio I *et al.* Self-renewing osteoprogenitors in bone marrow sinusoids can organize a hematopoietic microenvironment. *Cell* 2007; **131**: 324–336.
20. Xie H, Cui Z, Wang L, Xia Z, Hu Y, Xian L *et al.* PDGF-BB secreted by preosteoclasts induces angiogenesis during coupling with osteogenesis. *Nat Med* 2014; **20**: 1270–1278.
21. Thompson B, Towler DA. Arterial calcification and bone physiology: role of the bone-vascular axis. *Nat Rev Endocrinol* 2012; **8**: 529–543.
22. Burkhardt R, Kettner G, Böhm W, Schmidmeier M, Schlag R, Frisch B *et al.* Changes in trabecular bone, hematopoiesis and bone marrow vessels in aplastic anemia, primary osteoporosis, and old age: a comparative histomorphometric study. *Bone* 1987; **8**: 157–164.
23. Wang YX, Griffith JF, Kwok AW, Leung JC, Yeung DK, Ahuja AT *et al.* Reduced bone perfusion in proximal femur of subjects with decreased bone mineral density preferentially affects the femoral neck. *Bone* 2009; **45**: 711–715.
24. Mekraldi S, Lafage-Proust MH, Bloomfield S, Alexandre C, Vico L. Changes in vasoactive factors associated with altered vessel morphology in the tibial metaphysis during ovariectomy-induced bone loss in rats. *Bone* 2003; **32**: 630–641.
25. Ding WG, Wei ZX, Liu JB. Reduced local blood supply to the tibial metaphysis is associated with ovariectomy-induced osteoporosis in mice. *Connect Tissue Res* 2011; **52**: 25–29.
26. Driessens M. Circulatory aspects of reflex sympathetic dystrophy. In Schoutens A, Arlet J, Gardeniers JW, Hughes SPF (eds) *Bone Circulation and Vascularisation in Normal and Pathological Conditions.* Plenum Press: New York, 1993, pp 217–231.
27. Edwards JR1, Williams K, Kindblom LG, Meis-Kindblom JM, Hogendoorn PC, Hughes D *et al.* Lymphatics and bone. *Hum Pathol* 2008; **39**: 49–55.
28. Li XM, Hu Z, Jorgenson ML, Slayton WB. High levels of acetylated low density lipoprotein uptake and low tyrosine kinase with immunoglobulin and epidermal growth factor homology domains-2 (Tie2) promoter activity distinguish sinusoids from other vessel types in murine bone marrow. *Circulation* 2009; **120**: 1910–1918.
29. Wang L, Ciani C, Doty SB, Fritton SP. Delineating bone's interstitial fluid pathway *in vivo*. *Bone* 2004; **34**: 499–509.
30. Weiss L. Transmural cellular passage in vascular sinuses of rat bone marrow. *Blood* 1970; **36**: 189–208.
31. Zetterberg E, Vannucchi AM, Migliaccio AR, Vainchenker W, Tulliez M, Dickie R *et al.* Pericyte coverage of abnormal blood vessels in myelofibrotic bone marrows. *Haematologica* 2007; **92**: 597–604.
32. Branemark PI. Experimental investigation of microcirculation in bone marrow. *Angiology* 1961; **12**: 293–305.
33. Miller SC, Jee WSS. The microvascular bed of fatty bone marrow in the adult beagle. *Metab Bone Dis Rel Res* 1980; **2**: 239–246.
34. De Bruyn PP, Breen PC, Thomas TB. The microcirculation of the bone marrow. *Anat Rec* 1970; **168**: 55–68.
35. Bridgeman G, Brookes M. Blood supply to the human femoral diaphysis in youth and senescence. *J Anat* 1996; **188**: 611–621.
36. Roche B, David V, Vanden-Bossche A, Peyrin F, Malaval L, Vico L *et al.* Structure and quantification of microvascularisation within mouse long bones: what and how should we measure? *Bone* 2012; **50**: 390–399.
37. Horowitz M, Berry R, Webb R, NelsonT XiY, Doucette CR, Fretz JA *et al.* Bone marrow adipocytes are distinct from white or brown adipocytes. *J Bone Miner Res* 2014, S62: abstract FR0066.
38. Roche B, Vanden-Bossche A, Normand M, Malaval L, Vico L, Lafage-Proust MH. Validated laser doppler protocol for measurement of mouse bone blood perfusion - response to age or ovariectomy differs with genetic background. *Bone* 2013; **55**: 418–426.
39. Lassailly F, Foster K, Lopez-Onieva L, Currie E, Bonnet D. Multimodal imaging reveals structural and functional heterogeneity in different bone marrow compartments: functional implications on hematopoietic stem cells. *Blood* 2013; **122**: 1730–1740.
40. Spencer JA, Ferraro F, Roussakis E, Klein A, Wu J, Runnels JM *et al.* Direct measurement of local oxygen concentration in the bone marrow of live animals. *Nature* 2014; **508**: 269–273.
41. Wang L, Benedito R, Bixel MG, Zeuschner D, Stehling M, Sävendahl L *et al.* Identification of a clonally expanding haematopoietic compartment in bone marrow. *Embo J* 2013; **32**: 219–230.
42. Kunisaki Y, Bruns I, Scheiermann C, Ahmed J, Pinho S, Zhang D *et al.* Arteriolar niches maintain haematopoietic stem cell quiescence. *Nature* 2013; **502**: 637–643.
43. Méndez-Ferrer S, Michurina TV, Ferraro F, Mazloom AR, Macarthur BD, Sergio AL *et al.* Mesenchymal and haematopoietic stem cells form a unique bone marrow niche. *Nature* 2010; **466**: 829–834.
44. Ding L, Saunders TL, Enikolopov G, Morrison SJ. Endothelial and perivascular cells maintain haematopoietic stem cells. *Nature* 2012; **481**: 457–462.
45. Kusumbe A, Ramasamy S, Adams RH. Coupling of angiogenesis and osteogenesis by a specific vessel subtype in bone. *Nature* 2014; **507**: 325–328.
46. Sipkins DA, Wei X, Wu JW, Runnels JM, Côté D, Means TK *et al. In vivo* imaging of specialized bone marrow endothelial microdomains for tumour engraftment. *Nature* 2005; **435**: 969–973.
47. Hoggatt J, Mohammad KS, Singh P, Hoggatt AF, Chitteti BR, Speth JM *et al.* Differential stem- and progenitor-cell trafficking by prostaglandin E2. *Nature* 2013; **495**: 365–369.
48. Bränemark PI. Vital microscopy of bone marrow in the rabbit. *Scand J Clin Lab Invest* 1958; **11**: 1–82.
49. Mazo IB, Gutierrez-Ramos JC, Frenette PS, Hynes RO, Wagner DD, von Andrian UH. Hematopoietic progenitor cell rolling in bone marrow microvessels: parallel contributions by endothelial selectins and vascular cell adhesion molecule. *J Exp Med* 1998; **188**: 465–474.
50. Lo Celso C, Fleming HE, Wu JW, Zhao CX, Miake-Lye S, Fujisaki J *et al.* Live-animal tracking of individual haematopoietic stem/progenitor cells in their niche. *Nature* 2009; **457**: 92–96.
51. Köhler A, Schmithorst V, Filippi MD. Altered cellular dynamics and endosteal location of aged early hematopoietic progenitor cells revealed by time-lapse intravital imaging in long bones. *Blood* 2009; **114**: 290–298.
52. Trueta J, Morgan JD. The vascular contribution to osteogenesis. I. Studies by the injection method. *J Bone Joint Surg Br* 1960; **42-B**: 97–109.
53. Kelly PJ. Anatomy, physiology, and pathology of the blood supply of bones. *J Bone Joint Surg Am* 1968; **50**: 766–783.
54. Brookes M, Revell WJ. *Blood Supply of Bone.* Springer: London, 1998.
55. Pazzaglia UE, Bonaspetti G, Rodella LF, Ranchetti F, Azzola F. Design, morphometry and development of the secondary osteonal system in the femoral shaft of the rabbit. *J Anat* 2007; **211**: 303–312.
56. Horii T1, Matsumoto T, Nishino M, Tomita K. Effects of steroids on femoral diaphyseal intramedullary circulation in rabbits. *Arch Orthop Trauma Surg* 2002; **122**: 506–509.
57. Konerding MA1, Blank M. The vascularization of the vertebral column of rats. *Scanning Microsc* 1987; **1**: 1727–1732.
58. Boerckel JD, Uhrig BA, Willett NJ, Huebsch N, Guldberg RE. Mechanical regulation of vascular growth and tissue regeneration in vivo. *Proc Natl Acad Sci USA* 2011; **108**: E674–E680.
59. Nyangoga H, Mercier P, Libouban H, Baslé MF, Chappard D. Three-dimensional characterization of the vascular bed in bone metastasis of the rat by microcomputed tomography (MicroCT). *PLoS One* 2011; **6**: e17336.
60. Cao X, Wu X, Frassica D, Yu B, Pang L, Xian L *et al.* Irradiation induces bone injury by damaging bone marrow microenvironment for stem cells. *Proc Natl Acad Sci USA* 2011; **108**: 1609–1614.
61. Langer M, Prisby R, Peter Z, Boistel R, Lafage-Proust MH, Peyrin F. Quantitative investigation of bone microvascularization from 3D synchrotron micro-computed tomography in a rat model. *Conf Proc IEEE Eng Med Biol Soc* 2009; **2009**: 1004–1007.
62. Schneider P, Krucker T, Meyer E, Ulmann-Schuler A, Weber B, Stampanoni M *et al.* Simultaneous 3D visualization and quantification of murine bone and bone vasculature using micro-computed tomography and vascular replica. *Microsc Res Tech* 2009; **72**: 690–701.
63. Duvall CL, Taylor WR, Weiss D, Guldberg RE. Quantitative microcomputed tomography analysis of collateral vessel development after ischemic injury. *Am J Physiol Heart Circ Physiol* 2004; **287**: H302–H310.
64. Fei J, Peyrin F, Malaval L, Vico L, Lafage-Proust MH. Imaging and quantitative assessment of long bone vascularization in the adult rat using microcomputed tomography. *Anat Rec* 2010; **293**: 215–224.
65. Prisby R, Guignandon A, Vanden-Bossche A, Mac-Way F, Linossier MT, Thomas M *et al.* Intermittent PTH(1-84) is osteoanabolic but not osteoangiogenic and relocates bone marrow blood vessels closer to bone-forming sites. *J Bone Miner Res* 2011; **26**: 2583–2596.

66. Palacio-Mancheno PE, Larriera AI, Doty SB, Cardoso L, Fritton SP. 3D assessment of cortical bone porosity and tissue mineral density using high-resolution μCT: effects of resolution and threshold method. *J Bone Miner Res*, 2014; 29: 142–150.
67. Roche B, Vanden-Bossche A, Malaval L, Normand M, Jannot M, Chaux R *et al.* Parathyroid hormone 1-84 targets bone vascular structure and perfusion in mice: impacts of its administration regimen and of ovariectomy. *J Bone Miner Res* 2014; **29**: 1608–1618.
68. Vermeulen PB, Gasparini G, Fox SB, Colpaert C, Marson LP, Gion M *et al.* Second international consensus on the methodology and criteria of evaluation of angiogenesis quantification in solid human tumours. *Eur J Cancer* 2002; **38**: 1564–1579.
69. Van Valckenborgh E, De Raeve H, Devy L, Blacher S, Munaut C *et al.* Murine 5T multiple myeloma cells induce angiogenesis in vitro and in vivo. *Br J Cancer* 2002; **86**: 796–802.
70. Ellis SL, Grassinger J, Jones A, Borg J, Camenisch T, Haylock D *et al.* The relationship between bone, hemopoietic stem cells, and vasculature. *Blood* 2011; **118**: 1516–1524.
71. Hoggatt J, Mohammad KS, Singh P, Hoggatt AF, Chitteti BR, Speth JM *et al.* Differential stem- and progenitor-cell trafficking by prostaglandin E2. *Nature* 2013; **495**: 365–369.
72. Singbrant S, Russell MR, Jovic T, Liddicoat B, Izon DJ, Purton LE. Erythropoietin couples erythropoiesis, B lymphopoiesis, and bone homeostasis within the bone marrow microenvironment. *Blood* 2011; **117**: 5631–5642.
73. Jilka RL, O'Brien CA, Bartell SM, Weinstein RS, Manolagas SC. Continuous elevation of PTH increases the number of osteoblasts via both osteoclast-dependent and -independent mechanisms. *J Bone Miner Res* 2010; **25**: 2427–2437.
74. Schneider P, Stauber M, Voide R, Stampanoni M, Donahue LR, Müller R. Soft Tissue and Phase Contrast Imaging at the Swiss Light Source. In: MJ Yaffe, MJ Flynn (eds). Proceedings of SPIE on Medical Imaging 2004: Physics of Medical Imaging; 6 May 2004; San Diego, CA, USA. SPIE. 2004, pp 281–291.
75. Cooper DM, Turinsky AL, Sensen CW, Hallgrímsson B. Quantitative 3D analysis of the canal network in cortical bone by micro-computed tomography. *Anat Rec B New Anat* 2003; **274**: 169–179.
76. Pusztaszeri MP, Seelentag W, Bosman FT. Immunohistochemical expression of endothelial markers CD31, CD34, von Willebrand factor, and Fli-1 in normal human tissues. *J Histochem Cytochem* 2006; **54**: 385–395.
77. Soki FN, Li X, Berry J, Koh A, Sinder BP, Qian X *et al.* The effects of zoledronic acid in the bone and vasculature support of hematopoietic stem cell niches. *J Cell Biochem* 2013; **114**: 67–78.
78. Coenegrachts L, Maes C, Torrekens S, Van Looveren R, Mazzone M, Guise TA *et al.* Anti-placental growth factor reduces bone metastasis by blocking tumor cell engraftment and osteoclast differentiation. *Cancer Res* 2010; **70**: 6537–6547.
79. Anghelina M, Moldovan L, Moldovan NI. Preferential activity of Tie2 promoter in arteriolar endothelium. *J Cell Mol Med* 2005; **9**: 113–121.